J Solid State Electrochem (2008) 12:1497–1502
DOI 10.1007/s10008-008-0511-9

ORIGINAL PAPER

PVDF-HFP composite polymer electrolyte with excellent electrochemical properties for Li-ion batteries

Hui Xie · Zhiyuan Tang · Zhongyan Li · Yanbing He · Yong Liu · Hong Wang

Received: 9 October 2007 / Revised: 19 December 2007 / Accepted: 30 December 2007 / Published online: 17 January 2008

Abstract Poly (vinylidene fluoride-co-hexafluoropropylene)-based composite polymer electrolyte (CPE) was prepared by phase inversion technique. In this work, we first applied a novel surface-modified sub-micro-sized alumina, PC-401, as ceramic filler. Various electrochemical methods were applied to investigate the electrochemical properties of the polymer electrolytes. We found that the CPE with 10 wt.% PC-401 has excellent electrochemical properties, including the ionic conductivity as high as 0.89 mS cm^{-1} and the Li-ion transference number of 0.46. Polymer Li-ion batteries using $LiFePO_4$ as cathode active material exhibited excellent cycling and high-temperature performances. PC-401 shows a promising applicability in the preparation of polymer electrolyte with high electrochemical properties.

Keywords PVDF-HFP · Composite polymer electrolytes · Phase inversion · Li-ion battery · Transference number

Introduction

Polymer electrolyte separators have already found their application in polymer Li-ion batteries. Such batteries are expected to offer safe and reliable performance for hybrid electric vehicles and domestic applications. However, disadvantages like relatively low ionic conductivity, poor mechanical strength, and poor interfacial properties of the polymer electrolyte separators still prevent their application in power sources [1, 2]. The power capability of Li-ion battery with polymer electrolyte separator is still greatly limited by the low transference number of Li^+ in polymer electrolyte separators. Plasticized or gel polymer electrolyte (GPE) has attracted much attention since it exhibits high ionic conductivity by immobilizing large amount of liquid electrolyte in the polymer host [3]. However, the conductivity and mechanical stability of GPE are mutual exclusive, i.e., an enhancement in conductivity is achieved at the expense of reduced mechanical strength and vice versa [4]. Fortunately, the problems can be effectively circumvented by incorporating ceramic filler into the polymer matrix [5]. The addition of nano- or sub-micro-sized ceramic filler can suppress the crystallization of the polymer host and perform as a 'solid plasticizer', and hence, improve the ionic conductivity and maintain the mechanical strength, simultaneously [6–8].

Poly (vinylidene fluoride-co-hexafluoropropylene) (PVDF-HFP) is one of the most promising host matrices for polymer electrolytes because of its various appealing properties like high dielectric constant (ε=8.4), low crystallinity, and glass transition temperature (T_g) [1, 7–10]. Phase inversion has been a well-known technology for preparing microporous polymer electrolyte [11–13]. However, conventional phase inversion technology is based on the exchange between solvent and non-solvent, i.e., coagulation medium. This process significantly increases the cost and time of the membrane preparation. Then, evaporation phase inversion was proposed [14]. In this process, both solvent and non-solvent are used to "dissolve" the copolymer and ceramic filler. The membrane is dried after coated on a substrate to complete the preparation of the membrane. The alternate evaporation of and the exchange between solvent and non-

H. Xie (✉) · Z. Tang · Y. He · Y. Liu · H. Wang
School of Chemical Engineering and Technology,
Tianjin University,
Tianjin 300072, People's Republic of China
e-mail: xie.ziren@gmail.com

Z. Li
McNair Technology Co., Ltd.,
Dongguan City, Guangdong 523700, People's Republic of China

solvent produce the micropores. The distribution and size of the micropores can be controlled by the ratio of the two solvents and the evaporating temperature. This process is more effective and cost saving. In this paper, we chose acetone and ethanol, respectively, as solvent and non-solvent because they are miscible and have a different boiling point.

Fumed alumina PC-401 is a sub-micro-sized particle which has already been applied as a flow agent and light diffuser in cosmetics. It possesses unique cationic surface charge and hydrophilic surface activity. The aggregate size is microlevel (D95=0.3 μm). To date, there is no report available on applying PC-401 as a ceramic filler in polymer electrolyte separator. In this work, we introduced PC-401 into the PVDF-HFP polymer matrix as a ceramic filler and systematically investigated the effect of PC-401 on the electrochemical properties of polymer electrolyte by applying various electrochemical methods. We also studied the fabrication and electrochemical properties of the separator and evaluated its application in rechargeable Li/$LiFePO_4$ battery.

Experimental

PVDF-HFP (Kynar Flex™ 2801, Elf Atochem with HFP content of 12%) and PC-401 (Cabot) were dried in a vacuum oven at 120 °C for 24 h prior to use. The selected electrolyte of 1 M $LiPF_6$ in 1:1:1 (wt.%) EC–DMC–EMC was provided gratis by Tinci, China. An appropriate amount of PVDF-HFP was added into the mixture of acetone and ethanol (the weight ratio was: PVDF-HFP/acetone/ethanol=1:8:2). Different weight percent of PC-401 (i.e., ratio to the weight of PVDF-HFP), viz. 0, 5, 8, 10, and 15 wt.% were added. The suspension was magnetically stirred at 45 °C for 3–4 h and subsequently cast onto a newly cleaned glass plate using a doctor blade with a gap of 450 μm. After dried at 80 °C for 5–6 h, the obtained membrane was punched into disks of 2 cm^2.

To measure the porosity of the obtained films, we immersed the films into 1-butanol for 2 h. The porosity (P) was determined using the following equation,

$$P = \frac{m_a/\rho_a}{m_a/\rho_a + m_p/\rho_p}$$

where ρ_a and ρ_p are the density of 1-butanol and the dried film, respectively; m_a and m_p are the weight of incorporated 1-butanol and the dried film, respectively. It should be mentioned that, in this work, to verify the reproducibility and minimize the variability of the obtained results, we assembled and tested more than three specimens for every group of physical and electrochemical measurement.

The electrolyte uptake of the film was determined by calculating the ratio of the weight of electrolyte absorbed to the weight of the dry film. To measure this, we immersed the films into the selected electrolyte for 2 h.

The dry films were activated by immersing into the electrolyte solvent for more than 2 h before the electrochemical properties were investigated. The separator was sandwiched between two stainless steel (SS) blocking electrodes to determine the ionic conductivity. The diameter of the SS plates was 1 cm, that is, the effective electrode area of the blocking cell was calculated to be 0.785 cm^2. The SS plates were finely polished before the cell assembly. The conductivity (σ) of the separator was determined by AC impedance applied to the symmetric SS/SS cell.

Cells with a configuration of Li/SS were assembled to measure the electrochemical stability window of the separator by linear sweep voltammetry (LSV). Lithium metal was used as counter and reference electrode, and SS plate as working electrode. The voltage range of LSV measurement was from 2 to 5.5 V vs Li^+/Li.

The lithium-ion transference number (T_{Li}^+) of the CPE was measured by the method proposed by Bruce and Vincent [15, 16]. A DC polarization pulse of 10 mV was applied to the non-blocking, symmetric Li/CPE/Li cell. The current density loss was detected by DC chronoamperometry. Also the AC impedance spectra before and after the DC polarization were measured. The T_{Li}^+ was calculated using the expression below:

$$T_{Li^+} = I_s(V - I_0R_0)/I_0(V - I_sR_s)$$

The compatibility of the CPE with lithium metal was investigated by monitoring the time dependence of the impedance of the Li/CPE/Li cells.

Nano-structured $LiFePO_4$ material was prepared using sol–gel method described elsewhere [17] and used as the cathode active material. The cathode composite electrodes were prepared with a formulation of 80% (wt.) of active material, 10% carbon black as conductive additive and 5% PTFE as binder. The electrode load was 10 mg cm^{-2}. $LiFePO_4$/CPE/Li 2032-type button cells were assembled, and the cycling performance at room temperature and at 60 °C was tested. The cycling test was performed between the voltage of 2.5 and 4.2 V at 0.1 C.

All the electrochemical measurements were conducted by a Gamry Instrument (model PC4-750). The EIS of the cells was measured over the frequency range from 300 kHz to 0.1 Hz with an AC oscillation of 5 mV. The ZsimpWin™ software was used to analyze the obtained EIS plots.

Results and discussion

Ionic conductivity

Figure 1 presents the relationship of porosity and electrolyte uptake of the films with different contents of PC-401. It

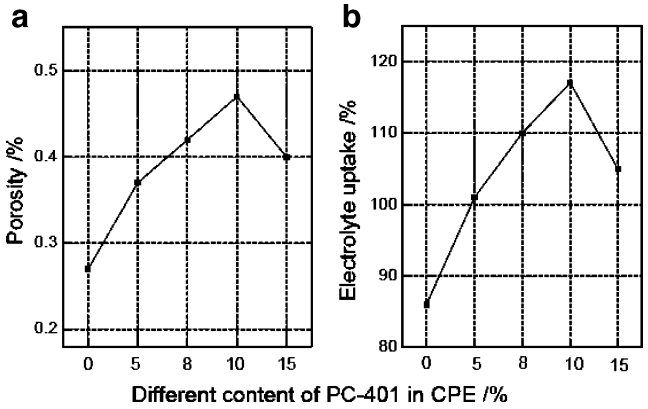

Fig. 1 The porosity (**a**) and electrolyte uptake (**b**) of the polymer films with different contents of PC-401

is clearly shown that by the addition of PC-401, the porosity and electrolyte uptake of the polymer film increase over the entire concentration range. The porosity keeps on increasing with the increase of PC-401 content and reaches a maximum with 10% PC-401 incorporated. It is a well-known fact that the addition of ceramic filler into the polymer electrolyte is an effective way to generate micro-pores in the polymer matrix [1, 18]. The porosity starts to decrease while more filler is added. The porosity with 15% PC-401 is much lower than that with 10%. This fact may be ascribed to the aggregation effect of the ceramic filler at high concentration levels. The behavior of electrolyte uptake is similar to that of the porosity, as shown in Fig. 1b. The uptake of FFPE is 86% and increases to 117% with 10% PC-401. The uptake is depressed to 105% when 15% PC-401 is added. The increase of electrolyte uptake is a combined result of the increase of porosity and the excellent affinity of the ceramic filler to polar organic solvents.

The trend of ionic conductivity of the film with different contents of PC-401 shown in Fig. 2 is well consistent with

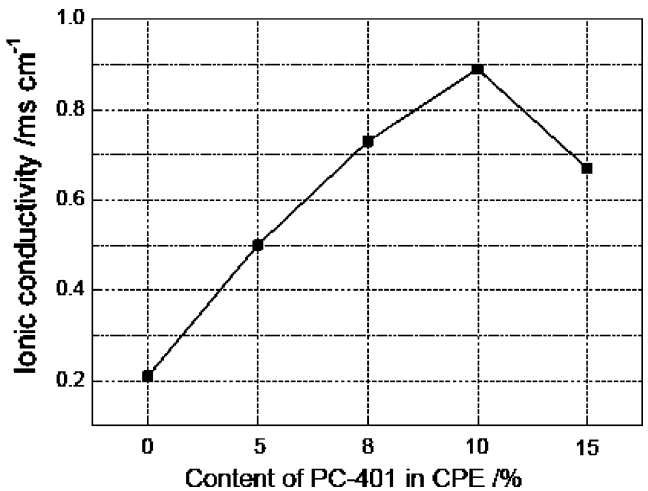

Fig. 2 The ionic conductivity of polymer electrolyte with different contents of PC-401 at room temperature

that of the porosity and electrolyte uptake. The enhancement of conductivity by adding PC-401 to the polymer matrix is a combined result of many respects. First, the improvement of ionic conductivity is mainly promoted by the high surface area of the PC-401 particles [5] and the increase of the uptake of liquid electrolyte into the PVDF-HFP matrix. The high surface area of PC-401 causes steric hindrance effect which favors fast ionic transport [19]. Second, the enhancement of ionic conductivity can be further interpreted in terms of Lewis acid–base interactions [19–21]. The cationic charges on the surface of PC-401 act as Lewis acid centers and compete with Li^+ cations (strong Lewis acid) to form complexes with the polymer host. This in turn may result in: (a) structural modifications and the promotion of Li^+-conducting pathways at the surface of filler, and (b) the lowering ionic coupling which promoting the salt dissociation [19]. These two effects would result in the promotion of "free" ions and account for the observed enhancement of the ionic conductivity in a wild temperature range.

Figure 3 compares the ionic conductivity vs temperature of the FFPE and CPE with 10% PC-401. A typical Vogel–Tamman–Fulcher (VTF) behavior [10, 22] is observed for both the FFPE and CPE. The VTF relationship well explains the transport properties in a viscous matrix.

The electrochemical stability window

To determine the electrochemical stability window of the CPE, linear sweep voltammetry (LSV) measurement was conducted using the Li/CPE/SS cell configuration and the obtained results are presented in Fig. 4. The obtained current

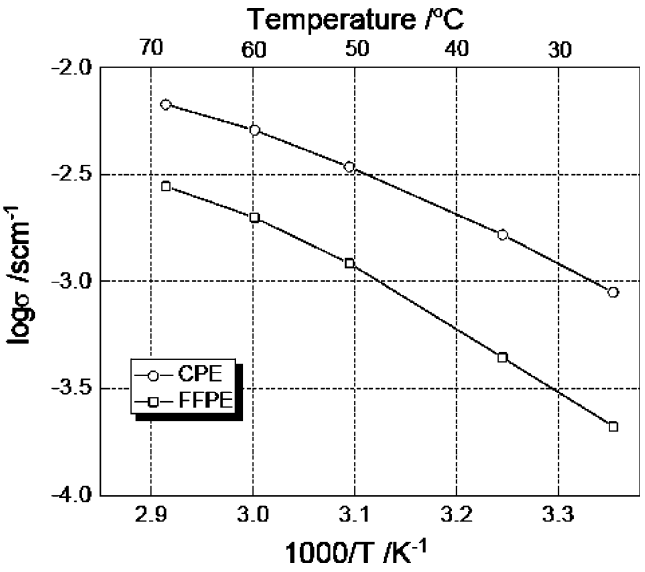

Fig. 3 Arrhenius curve of FFPE and CPE with 10% PC-401 from room temperature to 70 °C. It is shown that the ionic conduction of the polymer electrolyte obeys the VTF relationship

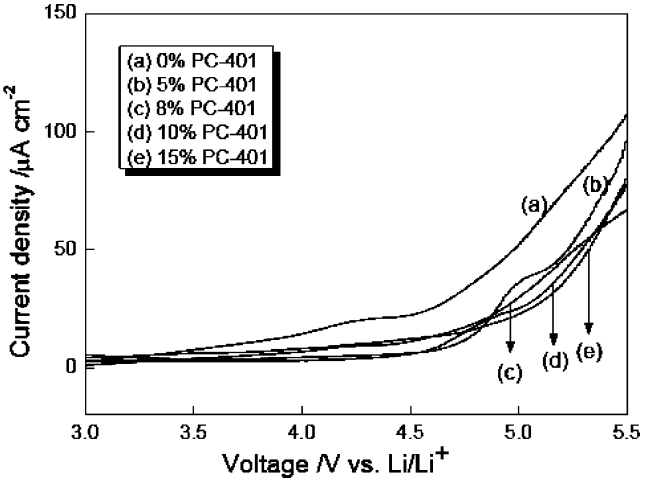

Fig. 4 The linear sweep voltammetry plots of SS/Li cells of polymer electrolyte with different filler contents

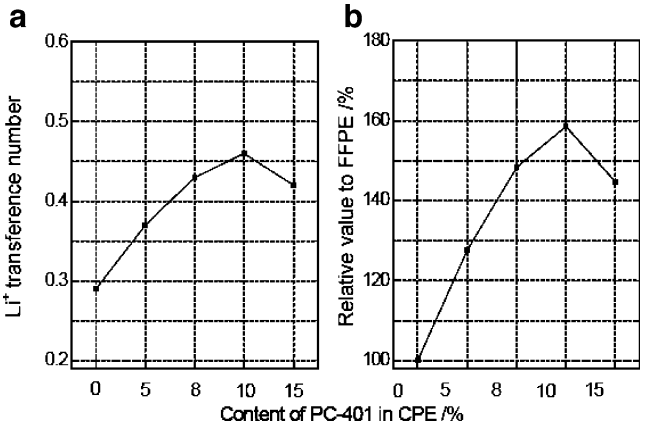

Fig. 5 The relationship of Li^+ transference number with the content of PC-401: **a** absolute value, **b** relative value to FFPE

density at lower voltages is the combined results of the ionic conductivity of the polymer electrolyte and the interfacial resistance of lithium metal/polymer electrolyte. Curve (*a*) presents a higher oxidative current density and indicates a stability window below 4.5 V vs Li/Li^+. One can clearly observe from curves (*b*)–(*e*) that the anodic current is significantly suppressed over the entire filler concentration, especially at high oxidative voltages. The composition voltage of polymer separator with PC-401 is higher than 4.7 V. This value is high enough to resist overcharge abuse in rechargeable Li-based batteries, which have a high working voltage by itself. It is interesting to note that there is no distinguished difference in electrochemical stability between CPEs with different filler contents. We consider that it is the intrinsic property of the ceramic filler to prevent the oxidative decomposition of both the polymer matrix and the incorporated electrolyte. The concentration of added filler only affects the relative value of the current density.

The Li-ion transference number

Lithium-ion transference number, T_{Li}^+, is one of the most important parameters for polymer electrolyte in Li-ion batteries [23–25]. The polarization due to concentration gradient in the cell is minimized if the fraction of current carried by lithium ion approaches unity. Hence, a relatively high T_{Li}^+ can effectively eliminate the concentration gradients within the batteries and ensure the working power density.

Figure 5 shows the relationship of T_{Li}^+ with the content of PC-401 added in the CPE. It is obvious that the addition of PC-401 can effectively increase the T_{Li}^+.

Since the obtained values may be equally affected by the passivation of the lithium metal surface, we reported the relative value of T_{Li}^+ to FFPE in Fig. 5(b) to clearly demonstrate the specific effect of PC-401 [19, 26]. This enhancement can also be interpreted in terms of Lewis acid–base theory. The Lewis acid sites on the surface of the ceramic filler could interact with both the polar atom in the polymer host and the anion of the lithium salt, hence weakening the interactions between these polar atoms and Li^+ and then releasing more free Li^+ to improve the T_{Li}^+ [2].

The compatibility with lithium metal

The compatibility of polymer electrolyte membranes with lithium metal or lighthearted graphite is still a remaining problem for the application in high power property Li-ion batteries. The reactivity of the anode electrode with electrolyte or polymer electrolyte can lead to an uncontrolled passivation process and results in the formation of a thick and non-uniform surface layer [27]. These can in turn cause an uneven lithium deposition during the charging process eventually leading to dentritic growth and cell short circuit [6]. Therefore, the interfacial property of lithium metal with polymer electrolytes plays a vital role in polymer Li batteries for practical application.

Figure 6 illustrates the time evolution of the impedance spectra of the CPE and FFPE, respectively. Figure 7 is the equivalent circuit model of the symmetric Li cell, where R_b and C_g are the bulk resistance and geometric capacity, which correspond to the arc at the highest frequency region. The depressed semicircle at the medium frequency is assigned to the combined effect of the resistance (R_{sei}) and capacitance (C_{sei}) of the interface on the surfaces of electrodes. R_{ct} and C_{dl} are the charge transfer resistance and its relative double-layer capacitance, which correspond to the semicircle at the relatively lower frequencies. As shown in Fig. 6, the R_b of the CPE cell was much lower and remained at a more stable value compared to the R_b of the FFPE cell. This observation can be ascribed to the higher and more stable ionic conductivity of the CPE. The compatibility of the polymer electrolyte and lithium metal is reflected by the time evolution of R_{sei} [28]. One can see

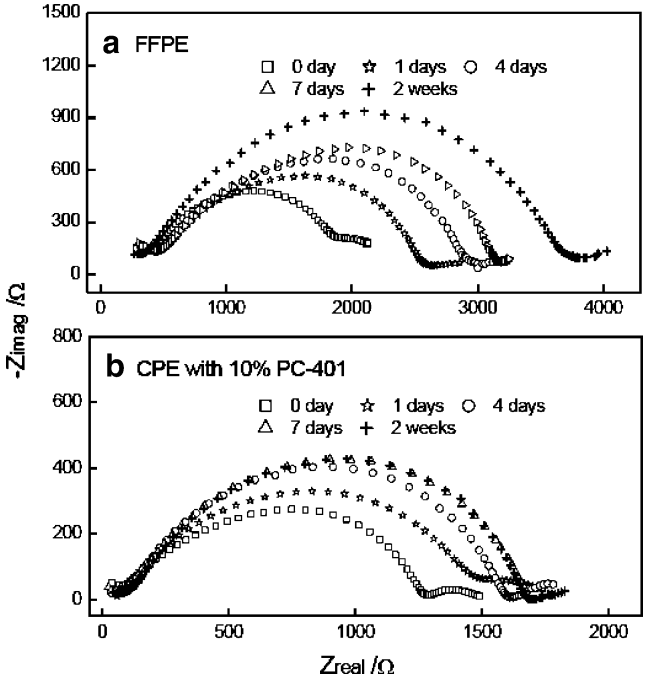

Fig. 6 Time evolution of the impedance spectra to investigate the compatibility of the polymer film with lithium metal

that the R_{sei} of the CPE increases in a much lower rate with storage time. The R_{sei} becomes stable within 2 weeks, whereas the R_{sei} increases obviously at that time. We consider that upon contact of the lithium metal with polymer electrolyte, chemical reactions between them take place. The resulting products accumulated on the surface of the lithium metal subsequently protecting them from further reactions [29]. Figure 6 compares the EIS plots of the two separators after a storage time of 2 weeks, the longest time we have tested. We can see that both the R_b and R_{sei} are much lower in CPE than in FFPE. The CPE is more conductive in polymer lithium batteries.

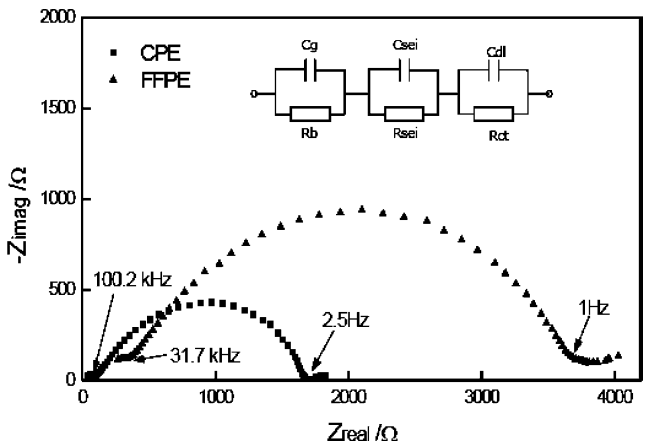

Fig. 7 Comparison of the EIS of the FFPE and CPE separator after stored for 2 weeks. Inset is the equivalent circuit model applied to analyze the data of EIS

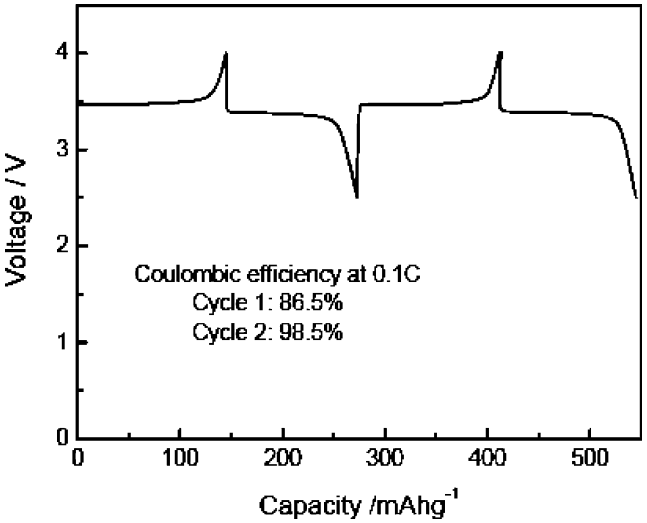

Fig. 8 Voltage–capacity curve of the initial two cycles of the Li/CPE/$LiFePO_4$ cell at 0.1 C rate

Performance of Li/CPE/$LiFePO_4$ cell

To further investigate the electrochemical properties of the as-prepared CPE, we assembled 2032 button cells applied $LiFePO_4$ as cathode active material and CPE with 10% PC-401 as separator electrolyte. Figure 8 shows the voltage–capacity curve of the first two cycles. The coulombic efficiency (CE) of the two cycles is calculated to be 86.5% and 98.5%, respectively. It is well known that the initial irreversibility of Li/cathode half-cells is associated with the reaction of electrolyte solvents with the lithium metal [30]. The relatively low CE of the first cycle is due to the formation of a necessary solid electrolyte interface (SEI) on the electrode surface. It is also related to the structural change of the cathode material and the irreversibly oxidative decomposition of the electrolyte solvents [31]. The value of 86.5% is rather high which suggests that the

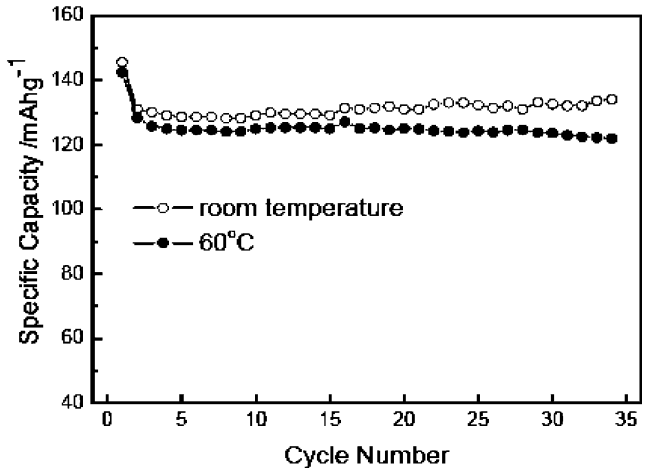

Fig. 9 Comparison of cycling performance of the polymer Li-ion cell with CPE at room temperature and at 60 °C

CPE doted with PC-401 is quite compatible with the lithium metal anode and the $LiFePO_4$ cathode.

The cycling performance of the cells at room temperature and at 60 °C is compared in Fig. 9. One can see that, except for the initial two cycles, both at room temperature and at 60 °C, the cells could cycle with an initial capacity of 125–130 mAh/g $LiFePO_4$ and retained excellent capacity retention. Slight capacity fading was exhibited while the temperature increased from room temperature to 60 °C. This fact verifies that the CPE separator can withstand high temperature of 60 °C without significant loss in mechanical strength. The addition of PC-401 can hybridize to strengthen the structure of the CPE separator and prevent it from being too fluid at elevated temperature [31].

Conclusions

In this work, by the addition of PC-401 into the PVDF-HFP polymer matrix, the polymer electrolyte membranes prepared by phase inversion technique show excellent electrochemical properties, such as high ionic conductivity, high stability window, and good compatibility with lithium metal. The $LiFePO_4$/Li cells using the membranes as separator cum electrolyte exhibit good cycling performance even at temperatures as high as 60 °C. Therefore, this nanocomposite polymer electrolyte is suitable for the application in polymer Li-ion batteries. The potential application of PC-401 deserves more attention to be explored as a ceramic filler into polymer electrolyte membrane for high performance polymer Li-ion batteries.

References

1. Wu C-G, Lu MI, Tsai C-C (2006) J Power Sources 159:295
2. Xi J, Qiu X, Ma X (2005) Solid State Ion 176:1249
3. Walkowiak M, Zalewska A, Jesionowski T, Pokora M (2007) J Power Sources 173:721
4. Ahmad S, Bohidar HB, Ahmad S, Agnihotry SA (2007) Polymer 47:3583
5. Croce F, Appetecchi GB, Persi L, Scrosati B (1998) Nature 394:456
6. Stephan AM, Nahma KS, Kulandainathanb MA, Ravic G, Wilsonc J (2006) Eur Polym J 42:1728
7. Stephan AM, Nahm KS, Kumar TP, Kulandainathan MA, Ravi G, Wilson J (2006) J Power Sources 159:1316
8. Stephan AM, Nahm KS (2006) Polymer 47:5952
9. Stolarska M, Niedzicki L, Borkowska R, Zalewska A, Wieczorek W (2007) Electrochim Acta 53:1512
10. Michael MS, Prabaharan SRS (2004) J Power Sources 136:408
11. Zhang SS, Xu K, Foster DL, Ervin MH, Jow TR (2004) J Power Sources 125:114
12. Wienk IM, Boom RM, Beerlage MAM, Bulte AMW, Smolders CA, Strathmann H (1996) J Membr Sci 113:361
13. Pasquier AD, Warren PC, Culver D, Gozdz AS, Amatucci GG, Tarascon J-M (2000) Solid State Ion 135:249
14. Pu W, He X, Wang L, Jiang C, Wan C (2006) J Membr Sci 272:11
15. Bruce PG (1995) Electrochim Acta 40:2077
16. Bruce PG, Vincent CA (1987) J Electroanal Chem 225:1
17. Choi D, Kumta PN (2007) J Power Sources 163:1064
18. Li Z, Su G, Wang X, Gao D (2005) Solid State Ion 176:1903
19. Croce F, Persi L, Scrosati B, Serraino-Fiory F, Plichta E, Hendrickson MA (2001) Electrochim Acta 46:2457
20. Appetecchi GB, Croce F, Persi L, Ronci F, Scrosati B (2000) Electrochim Acta 45:1481
21. Wieczorek W, Florjanczyk Z, Steve JR (1995) Electrochim Acta 40:2251
22. Aihara Y, Arai S, Hayamizu K (2000) Electrochim Acta 45:1321
23. Croce F, Persi L, Scrosati B, Fiory FS, Plichta E (2001) Electrochim Acta 46:2457
24. Croce F, Appetecchi GB, Persi L, Scrosati B (1998) Nature 394:456
25. Tarascon JM, Armand M (2001) Nature 414:359
26. Evans J, Vincent CA, Bruce PG (1987) Polymer 28:2324
27. Croce F, Scrosati B (1993) J Power Sources 43:9
28. Jiang Z, Carroll B, Abraham KM (1997) Electrochim Acta 42:2667
29. Zhang SS, Ervin MH, Xu K, Jow TR (2004) Electrochim Acta 49:3339
30. Zhang SS, Xu K, Jow TR (2003) Solid State Ion 1:58:375
31. Chojnacka J, Acosta JL, Morales E (2001) J Power Sources 97–98:819